IOP Conf. Series: Journal of Physics: Conf. Series **798** (2017) 012059 doi:10.1088/1742-6596/798/1/012059

Centrality determination in heavy-ion collisions with the CBM experiment

Klochkov[1,2], I Selyuzhenkov[2] for the CBM Collaboration

[1] Goethe University Frankfurt, Max-von-Laue-Straße 1, Frankfurt am Main, Germany
[2] GSI Helmholtzzentrum für Schwerionenforschung, Planckstraße 1, Darmstadt, Germany

E-mail: v.klochkov@gsi.de, ilya.selyuzhenkov@gmail.com

Abstract. The size and evolution of the medium created in a heavy-ion collision depends on collision geometry. Experimentally collisions can be characterized by the measured particle multiplicities around midrapidity or by the energy measured in the forward rapidity region, which is sensitive to the spectator fragments. In the Compressed Baryonic Matter (CBM) experiment at the future Facility for Antiproton and Ion Research (FAIR) the multiplicity of produced particles is measured with the silicon tracking system (STS). The projectile spectator detector (PSD) measures the energy of spectator fragments. We present the procedure of collision centrality determination in CBM and its performance using the PSD and the STS information.

1. Introduction

In heavy-ion collisions particle production and evolution of the medium created in the overlap region depends on the details of the initial geometry. At a given collision energy the initial energy density is defined by geometrical variables such as impact parameter (b), number of nucleon-nucleon collisions (N_{coll}) and number of participating nucleons (N_{part}). The dependence of different physics observables on the collision geometry is important for constraining parameters of heavy-ion collision models (see e. g. [1, 2]). Experimentally collisions are grouped into event (centrality) classes with the most central class defined by events with the highest multiplicity (smallest forward energy) which corresponds to small values of the impact parameter. Average geometrical quantities for different centrality classes are deduced from a Monte Carlo Glauber (MC-Glauber) model.

2. CBM simulation setup

CBM is a future fixed target experiment at FAIR. Its detector subsystems are shown in figure 1 (left) and includes Superconducting Dipole Magnet [3] (maximal magnetic field is 3.25 T), Micro-Vertex Detector (MVD), STS [4], Ring Imaging Cherenkov Detector (RICH) [5], Transition Radiation Detector (TRD), Time-of-Flight Wall (TOF) [6], Electromagnetic Calorimeter (ECal) [7] and PSD [8]. Tracking detectors MVD and STS have an acceptance in polar angle (Θ) $2.5^\circ < \Theta < 25^\circ$. The PSD has 44 modules elongated in x direction and covers the range in x (y) of $0.21^\circ < \Theta < 5.7^\circ$ (4.3°) at a distance of 8 m from the target which is optimized [8] for FAIR energy range $\sqrt{s_{NN}}$=2.7-4.8 AGeV. The PSD has a 6 cm hole in the center which is

needed to avoid radiation damage at high beam intensities expected at CBM. It is sensitive to spectator fragments (central modules) and produced particles (outer modules).

A sample of 1M Au+Au collisions with beam energy of 10 AGeV simulated with DCM-QGSM event generator (see [8] and references [18-28] therein) was used for the analysis. PSD was shifted horizontally in the transverse plane by 11 cm which account for the beam deflection in magnetic field with a bending power of 1 Tm. CBMROOT [9] is used to simulate the detector response to particles transported with GEANT4 [10] through the CBM setup. Charge particles tracks are reconstructed in STS and MVD. Event multiplicity (M_{trk}) calculated from tracks with at least 3 hits and a number of hits associated to the track more than 70% out of the total possible number for this track. The PSD modules were grouped into PSD1, PSD2 and PSD3 subgroups as shown in the figure 1 (right).

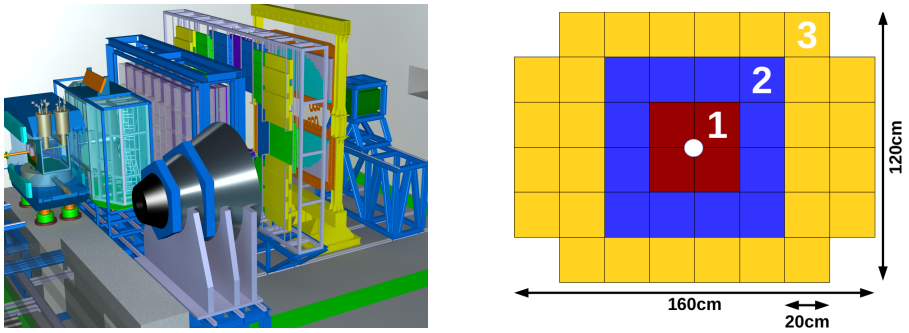

Figure 1. (left) Layout of the CBM experiment. (right) Transverse to the beam layout of the PSD modules. Colors show module subgroups used in the analysis: PSD1, PSD2 and PSD3.

3. Centrality determination procedure and performance

A Glauber model is commonly used to connect geometrical variables with measured quantities (e. g. particle multiplicity) [11]. In this approach the multiplicity of a heavy-ion collision is modeled as a sum of particles produced from a set of N_a independent emitting sources (ancestors). Each ancestor produces particles according to negative binomial distribution (NBD) with mean value μ and width σ

$$M_{\mathrm{Gl}}(N_a, \mu, \sigma) = P_{\mu,\sigma} \times N_a, \qquad N_a(f) = fN_{part} + (1-f)N_{coll}, \tag{1}$$

where N_{part} and N_{coll} are the number of participants and the number of binary collisions simulated with MC-Glauber corresponds to contributions from soft and hard processes.

The simulated multiplicity distribution for the CBM setup is then parameterised with a distribution of M_{Gl} simulated according to equation (1-2). The result of the procedure is shown in figure 2 (left). The MC-Glauber fit was done for multiplicities above 40. Dependence of the fit quality (χ^2) on σ and f for the best value of μ is shown in figure 2 (right). The minimum of the χ^2 corresponds to small contribution of hard processes (f=1). In reality it is very difficult to calculate total number of events which corresponds to the total inelastic cross-section due to the trigger inefficiencies or event selection, and contribution from electromagnetic processes. MC-Glauber fit can be used to estimate this number. A value of the multiplicity at which MC-Glauber fit starts to diviate from the multiplicity distribution defines the so called anchor point below which centrality determination is not reliable. The total number of events estimated with the MC-Glauber fit were found to be consistent with the total number of simulated events within 10%.

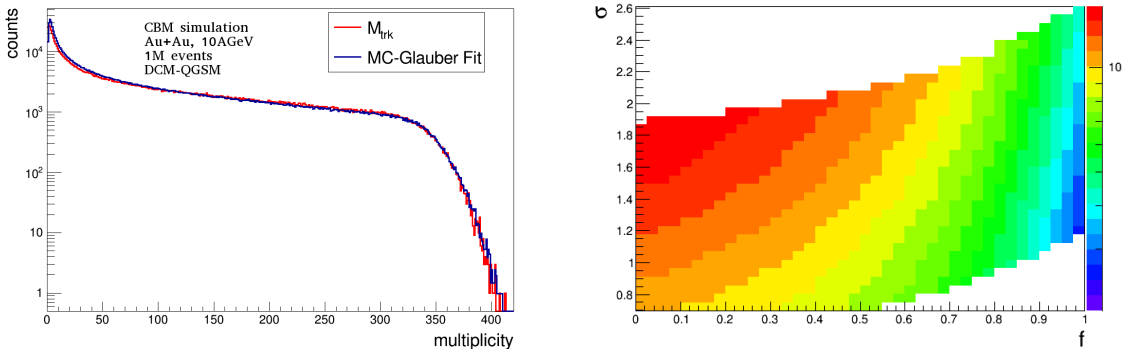

Figure 2. (left) Track multiplicity distribution obtained with DCM-QGSM and full CBM simulation compared to the fitted distribution using MC-Glauber. (right) MC-Glauber fit quality (χ^2) for different values of σ and f.

In figure 3 (left) centrality classes defined by selection on the track multiplicity are shown. Figure 3 (right) shows the resolution of impact parameter b which is defined as a ratio of a width of the b distribution σ_b to the impact parameter average $< b >$ in a given centrality class. Black triangles in figure 3 (right) show the resolution of impact parameter for track multiplicity estimator. It is in the range of 5-10% for mid-central and peripheral collisions.

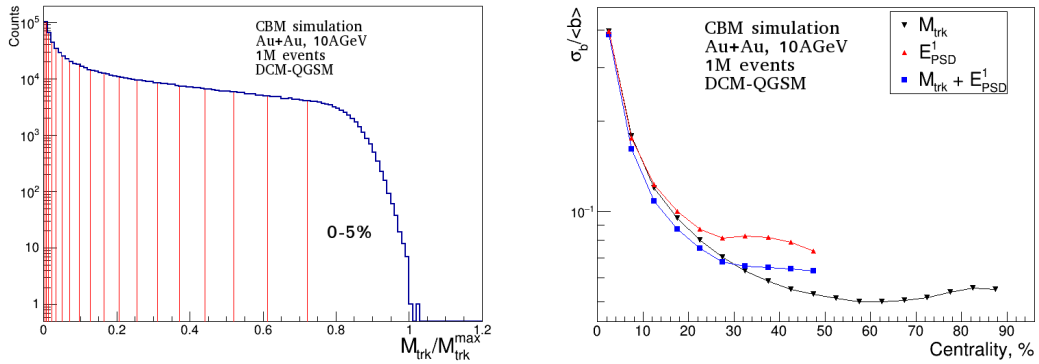

Figure 3. (left) Distribution of the track multiplicity normalized to its maximal value $M_{trk}^{max} = 404$. 5% centrality classes defined with MC-Glauber normalization are indicated with red lines. (right) Impact parameter resolution obtained with the same MC-Glauber normalization for different centrality estimators (track multiplicity, PSD energy and combined).

In figure 4 the impact parameter distribution extracted from MC-Glauber in different centrality classes is shown. The average impact parameter and the width of its distribution estimated with MC-Glauber are consistent with the values used in DCM-QGSM event generator within 5-10%. This difference increases for peripheral collisions.

The centrality determination with the PSD is comlicated due to the PSD hole. The impact of the hole on the correlation between the energy deposited in the central modules of PSD (E_{PSD}^1) and the track multiplicity is shown in figure 5 (left). For about 40% most peripheral events one or more fragments are missing, which leads to decorrelation between the measured energy and the geometrical quantities such as the impact parameter. Those events are removed from the analysis with a cut $M_{trk}/M_{trk}^{max} > 0.6 - 0.8E_{PSD}/E_{PSD}^{1,max}$ (shown by the red line in figure 5 left).

In figure 5 (right) centrality classes with forward rapidity energy is shown. Impact parameter resolution obtained with PSD1 is comparable to that of the STS for central (0-25%) events and

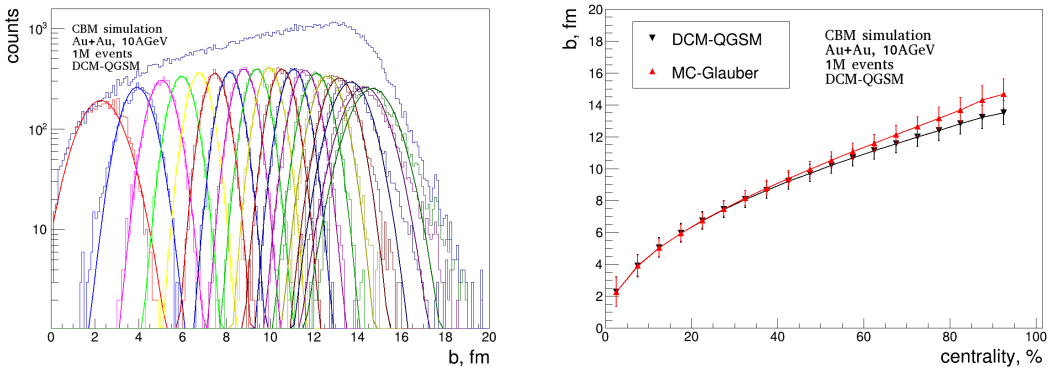

Figure 4. (left) Impact parameter distribution in different centrality classes. (right) Average impact parameter versus centrality. Errors show widht of b distribution.

significantly worse for centralities above 30% (figure 3 right, red triangles).

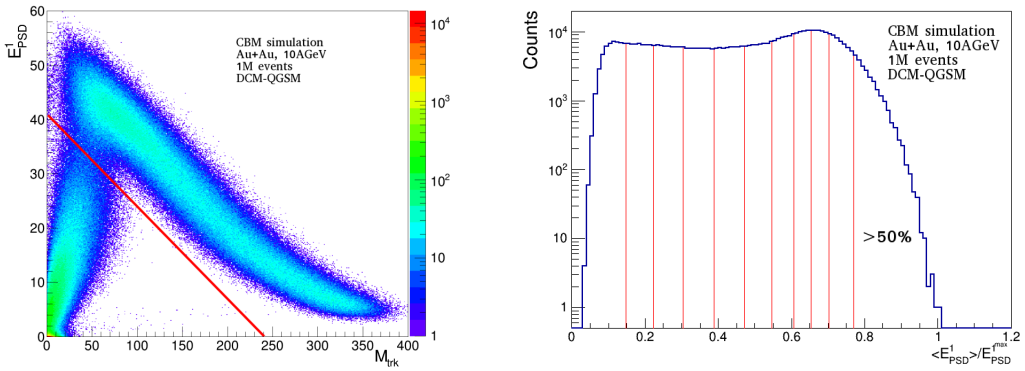

Figure 5. (left) The correlation between the energy deposited in the central PSD modules (E^1_{PSD}) and the track multiplicity M_{trk}. (right) Distribution of the energy deposited in the central PSD modules normalized to its maximal value $E^{1,max}_{PSD}$=60 GeV. 5% centrality classes defined with MC-Glauber normalization are indicated with red lines.

Centrality determination procedure using correlation between forward rapidity energy and track multiplicity is illustrated in figure 6. Using correlation between track multiplicity and PSD energy (figure 6 left) improves the impact parameter resolution in central (0-30%) collisions up to 10% (figure 3 right, blue squares).

Based on results presented in figures 2-6 the following automated procedure for event-by-event centrality determination was implemented for the CBMROOT:

(i) Determination of number of inelastic collisions and the anchor point using MC-Glauber fit.
(ii) Possibility to apply run-by-run corrections for variation of the average energy deposition in PSD subgroup and track multiplicity (to be used in future studies).
(iii) Scale M_{trk} and E_{PSD} by their maximal values (M^{max}_{trk} and E^{max}_{PSD}).
(iv) Parameterise correlation between multiplicity and/or energies of the PSD subgroup by following steps (see Fig. 6 right panel):
  (a) Profile the correlation horizontally (black circles) and fit with a polynomial function (black line);
  (b) Profile the correlation along the polynomial fit line (red squares) and refit (red line).

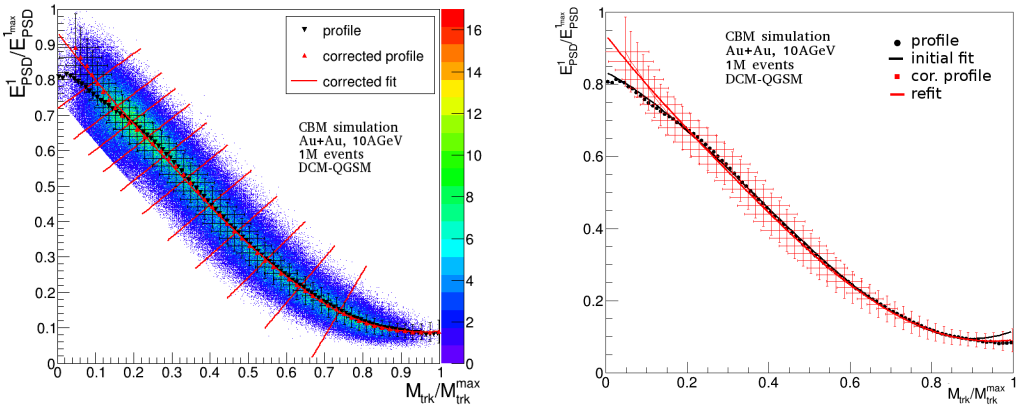

Figure 6. (left) The correlation between the energy deposited in the central modules of the PSD (PSD1) and track multiplicity with a cut $M_{trk}/M^{max}_{trk} > 0.6 - 0.8E_{PSD}/E^{1,max}_{PSD}$. (right) The result of the fit procedure (see text for details).

(v) Slice correlation perpendicular to the refit result (Fig. 6 left panel) or distribution (Fig. 6 left panel) in percentiles of total number of events obtained with MC-Glauber.

An experiment independent ROOT implementation of the algorithm was interfaced to CBMROOT. The same framework was also interfaced and tested with NA61/SHINE Pb+Pb test data [13].

4. Summary and outlook

Centrality Framework was developed and tested for the CBM setup. The centrality determination based on track multiplicity provides an impact parameter resolution of about 5-10% for mid-central and peripheral events. Based on the DCM-QGSM model simulations it was found that 40% of peripheral events have fragments missing in the PSD due to the beam hole which limit PSD centrality determination to 0-50%. The impact parameter resolution obtained with the PSD centrality estimation is comparable to that of the STS+MVD for centrality up to 30%. Note, that the DCM-QGSM model does not have realistic fragmentation of heavy-ion recoil. An extended version of this model is only available for collisions of light nuclei [14]. In future we plan to test MC-Glauber with sub-nucleon degrees of freedom [15] and extend MC-Glauber fitting procedure for energy in PSD and correlation.

References

[1] Adam J *et al.* [ALICE Collaboration] 2016 *Phys. Rev. Lett.* **116** 222302
[2] Aamodt K *et al.* [ALICE Collaboration] 2011 *Phys. Rev. Lett.* **106** 032301
[3] Malakhov A *et al.* [CBM Collaboration] *CBM SDM TDR* https://repository.gsi.de/record/109025
[4] Heuser J *et al.* [CBM Collaboration] *STS TDR* http://repository.gsi.de/record/54798
[5] Höhne C *et al.* [CBM Collaboration] *RICH TDR* http://repository.gsi.de/record/65526
[6] Herrmann N *et al.* [CBM Collaboration] *TOF TDR* http://repository.gsi.de/record/109024
[7] Korolko I [CBM Collaboration] *CBM ECal* these proceedings
[8] Guber F *et al.* [CBM Collaboration] *PSD TDR* http://repository.gsi.de/record/109059
[9] *CBMROOT, JUN16 release* https://redmine.cbm.gsi.de/projects/cbmroot/repository/show/release/JUN16
[10] *CERN, GEANT, Detector Description and Simulation Tool* https://geant4.web.cern.ch/geant4
[11] Abelev B *et al.* [ALICE Collaboration] 2013 *Phys. Rev. C* **88** 044909
[12] Bleicher M *et al.* 1999 *J. Phys.* G **25** 1859
[13] Aduszkiewicz A *et al.* [NA61/SHINE Collaboration], *Annual report* https://cds.cern.ch/record/2222876
[14] Botvina A S, Gudima K K and Pochodzalla J 2013 *Phys. Rev.* C **88** 054605
[15] Loizides C 2016 *Phys. Rev.* C **94** 024914